

A general frame for modeling the electrical propagation along graphene nanoribbons, carbon nanotubes and metal nanowires

A Maffucci^{1*}, G Miano²

¹*DIEI, University of Cassino and Southern Lazio, via G. Di Biasio 43, 03043 Cassino, Italy/INFN-LNF, Via E. Fermi 40, 00044, Frascati, Italy*

²*DIETI, University of Naples "Federico II", via Claudio 21, 80125, Naples, Italy*

*Corresponding author's e-mail: maffucci@unicas.it

Received 6 October 2014, www.cmnt.lv

Abstract

A general frame is proposed to model the propagation of electrical signals along nano-interconnects, either made by carbon nanotubes, graphene nanoribbons or metal nanowires. In the typical operating conditions of the next generations of integrated circuits, the electro-dynamics of the nano-interconnects may be conveniently described by means of a semi-classical transport model, based on the modified Boltzmann transport equation. From this model we derive here a generalized non-local dispersive Ohm's law, which can be regarded as the constitutive equation for the material. From the knowledge of the conduction and valence subbands, it is possible to define an equivalent number of conducting channels, which affects the circuit parameters of such interconnects. The study of the dispersion introduced by the generalized Ohm's law gives a clear explanation to the different propagation properties of nano-interconnects made by carbon materials and conventional metals.

Keywords: Carbon Nanotubes, Graphene nanoribbons, Metal nanowires, Nano-interconnects, Transmission lines

1 Introduction

Conventional materials so far used for microelectronics are not suitable for many nanoelectronics applications, because their performance does not meet the needed electrical, thermal and mechanical requirements. Therefore, a strong innovation is required, which may come either from the use of conventional materials with new structural arrangements, or by the use of innovative materials. Due to their outstanding physical properties, two possible allotropes of carbon are candidates to replace conventional materials in future nanoelectronics: the *graphene* (a graphite layer) and the *carbon nanotube* (a rolled-up version of graphene). Both materials exhibit low electrical resistivity, high thermal conductivity, high current carrying capability, besides other excellent mechanical properties [1, 2].

This is the main reason why, in the recent years, many efforts of the scientific community were devoted to the so-called *carbon electronics* [3, 4]. The fabrication of bundles of carbon nanotubes (CNTs) has reached satisfactory levels in terms of density, direction control, CMOS compatibility and contact resistance [5]. As for the graphene nanoribbons (GNRs), excellent results have been obtained for good quality large-scale fabrication [6]. The first real world applications became a reality, and so graphene and carbon nanotubes are now considered major candidates to become the silicon of the 21st century [7, 12]. The first examples of successful use of carbon-based nano-interconnects in IC technology have recently been demonstrated. The works [13] and [14] present high frequency CMOS oscillators integrating CNT or GNR interconnects, whereas [15] shows the first example of a computer with PMOS transistors entirely made by CNTs. Carbon or graphene interconnects are also successfully integrated into innovative organic transistors for the flexible plastic electronics [16]. As already pointed out, conventional materials are expected to fail in meeting

the performance requested to nano-interconnects enabling the transmission of clock, data and power in future nanoelectronics. From the electrical point of view, the main limitations expected when scaling down the conventional copper conductors to nanoscale dimensions come from the increasing electrical resistivity and insufficient current carrying capability [17].

An alternative solution to the use of new materials may come from the use of conventional materials, with new arrangements at nanoscale. An example is given by the metallic nanowires (NWs) which are made by metal atoms arranged in 1-D structures instead of the conventional 3D crystalline counterparts. Nanowires exhibit typical cross section sizes of the order of the material mean free path (some nanometers), and aspect ratios of 1000 or more. Conducting and semiconducting nanowires are proposed for nano-device applications [18], for molecular electronics [19], and in particular for interconnect applications [20].

A common feature for nanowires, carbon nanotubes and graphene nanoribbons is that the characteristic dimensions of transverse section are negligible compared to the longitudinal length. In other words, they can be regarded as one-dimensional (1-D) materials, for which the electrical conduction is characterized by two quantum-confined directions and one unconfined one. Based on this common feature, this paper shows how it is possible to derive a general frame to model the electrical propagation along nano-interconnects made by such materials.

The increasing interest in nano-interconnects leads to the quest for more and more accurate and reliable models, able to include all the quantum effects arising at nanoscale. This topic has been given a large attention by the recent literature, which presented several modeling approaches, like phenomenological [21] and semi-classical ones [22]. Based on such models, many papers predicted that carbon materials could outperform copper for IC on-chip interconnects and

vias [23-26].

In the typical working conditions of nano-interconnects, namely, frequency up to THz and low bias conditions, such nano-structures do not exhibit tunneling transport. Thus, the electrostatics may be studied by using a semi-classical description of the electron transport. This leads to the derivation of a constitutive relation between the electrical field and the density of the current in the form of a generalization of the classical Ohm's law, introducing non-local interactions and dispersion. By coupling such a relation to Maxwell equations, it is possible to derive a generalized transmission line model for such nano-interconnects. This approach has been adopted for modeling isolated metallic CNTs in [27], CNTs with arbitrary radius and chirality [28], multi-walled CNTs [29], and GNRs [30]. The semi-classical model gives results consistent with those provided by an alternative hydrodynamic model [31].

Here the formulation is extended to include nanowires of conventional metals, and a general expression is given for the constitutive relation of any nano-interconnect made by such 1D materials, Section 2. A key figure of the model is given by the effective number of conducting channels, which affects directly the parameters of the equivalent circuit models for the nano-interconnects, such as the conductance or the inductance. Section 2 presents a detailed discussion on the comparison between 1D structures made by CNT or GNRs and those made by conventional materials.

In Section 3 the propagation properties are investigated and the effects of the dispersion and quantum phenomena are discussed, referring to the phase velocity and the attenuation constant.

2 Generalized Ohm's law for 1D nano-conductors

The reference problem is depicted in Fig.1: a nano-interconnect is considered, made by a signal conductor above a perfect conducting ground (the presence of a dielectric is omitted). In the circular arrangement, the signal conductor is made by a single-wall CNT or by a conventional NW, whereas in the microstrip-like configuration the signal trace is made by a GNR. The starting point for the analysis of the electromagnetic behavior of such a structure is an accurate description of the electrostatic behavior, aimed at deriving a constitutive relation between the density of electrical current and the electrical field.

At macroscopic scale, which means for dimensions of hundreds of nanometers and greater, conventional conductors are studied by means of the classical electron transport model where the charges are treated as atoms in gas, which undergo random thermal motion with an average thermal velocity and a direct motion, characterized by the drift velocity. This approach leads to the classical Ohm's law, that reads in frequency domain:

$$J_z(z, \omega) = \sigma_c(\omega) E_z(z, \omega), \quad (1)$$

where $\sigma_c(\omega)$ is the Drude conductivity

$$\sigma_c(\omega) = \frac{\sigma_0}{1 + i\omega/\nu}, \quad (2)$$

being ν the collision frequency and σ_0 the DC value. In (1) and (2) we considered the simplified case where the

macroscopic motion is aligned along the conductor axis z .

On the opposite, at the molecular or atomic scale a quantum mechanical description is needed, since the transport is characterized by the wave-like behavior of electrons, where tunneling is possible. The Schrödinger equation is the basis for modeling the electrostatics: a Schrödinger/Maxwell model would take rigorously into account the quantum nature of the transport, but would easily lead to unaffordable numerical problems when increasing the number of carriers.

The cross-section sizes of the 1-D structures of our interest are typically large enough (at least 1 nm in the quantum confined directions) to have local crystal structures and to allow using a third approach, the *semi-classical transport model*. The electrons are classical particles but the movement takes place in a spatially periodic potential, where they move between two collisions according to the Boltzmann transport equation. Electrons behave like particles, unable to tunnel through barriers. In the collision events, the electrons can scatter inelastically, and so the kinetic energy of an incident particle is not conserved.

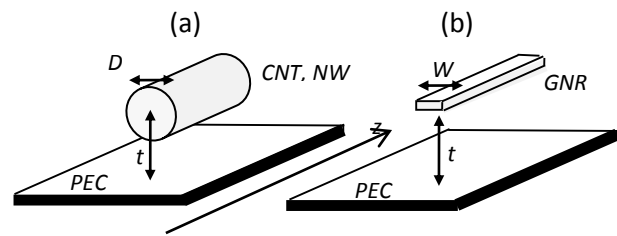


FIGURE 1 Reference geometry for the nano-interconnect: signal conductor made by (a) CNT or NW; (b) a GNR

2.1 TRANSPORT EQUATION

In any of the 1-D materials considered here, the electrons are quantum confined laterally and thus occupy quantized energy levels, instead of the traditional continuum of energy levels or bands that can be found in bulk materials. Along the longitudinal axis, the lattice exhibits translational symmetry and is long enough that the set of the possible values of the longitudinal wave-number k may be assumed to be almost continuous. The procedure presented here starts from the knowledge of the energy subbands for such materials: as pointed out before, they are quantized, so may be labeled by a band index μ and a wave vector $\mathbf{k} = k\mathbf{u}$, where \mathbf{u} is the unit vector oriented along the material lattice.

The subbands for CNTs and GNRs may be found by using the so-called *tight-binding approximation*, as shown in [32-34], whereas for metal nanowires it is possible to resort to calculations made by first principles [35].

Figure 2 shows some typical distributions of energy bands as functions of the wavenumber, for copper nanowire, metallic GNRs, and metallic CNTs.

Let us consider operating frequencies up to some THz, so that:

1. the cross section typical dimension (D or W , see Fig.1) is electrically small;
2. the transverse currents may be neglected;
3. only intraband transitions are considered, whereas interband ones are not allowed.

In these conditions, the longitudinal transport may be studied by considering the carrier transport for each of the n

subbands, either the conduction (+) and the valence (-) ones.

Let us indicate with $f_{\mu}^{(\pm)}$ the distribution function associated to the generic μ -th subband $E_{\mu}^{(\pm)}$: the carrier velocity is given by:

$$v_{\mu}^{(\pm)}(k) = \frac{dE_{\mu}^{(\pm)}}{d(\hbar k)}, \quad (3)$$

being \hbar the Planck constant. The transport may be modeled by the semi-classic Boltzmann equations [28, 29]:

$$\frac{\partial f_{\mu}^{(\pm)}}{\partial t} + v_{\mu}^{(\pm)} \frac{\partial f_{\mu}^{(\pm)}}{\partial z} + \frac{e}{\hbar} E_z \frac{\partial f_{\mu}^{(\pm)}}{\partial k} = -v (f_{\mu}^{(\pm)} - f_{0,\mu}^{(\pm)}), \quad (4)$$

where e is the electron charge, E_z is the longitudinal component of the electric field at the interconnect surface, whereas $\nu = v_F / l_{mfp}$ is the collision frequency, being l_{mfp} the mean free path and v_F the Fermi velocity.

The distribution function at equilibrium may be expressed as:

$$f_{0,\mu}^{(\pm)}(k) = F[E_{\mu}^{(\pm)}(k)] / X, \quad (5)$$

where $F[E]$ is the Dirac-Fermi distribution function

$$F[E] = \frac{1}{e^{E/k_B T} + 1}, \quad (6)$$

and

$$X = \begin{cases} D & \text{for CNT} \\ \pi W & \text{for GNR} \\ \pi(D/2)^2 & \text{for NW} \end{cases}, \quad (7)$$

being k_B the Boltzmann constant and T the absolute temperature. Note that the parameter X in (7) is a length for CNTs and GNRs, and an area for the nanowire. The reason for this difference resides in the fact that the density of electrical current J_z is given in A/m for CNTs and GNRs and in A/m² for solid NWs, as shown later.

2.2 GENERALIZED OHM'S LAW

Let us consider time-harmonic electric field $E_z(z,t) = \text{Re}\{\hat{E}_z \exp[i(\omega t - \beta z)]\}$ and current density $J_z(z,t) = \text{Re}\{\hat{J}_z \exp[i(\omega t - \beta z)]\}$, where β is the axial wavenumber.

In the low bias limit, namely for voltage values $V < k_B T / e$, we can assume small perturbations around the equilibrium:

$$f_{\mu}^{(\pm)}(k) = f_{0,\mu}^{(\pm)}(k) + \delta f_{\mu}^{(\pm)}(k, \beta, \omega) \quad (8)$$

and solve in the wave-number and frequency domain a linearized version of the transport equation (4), obtaining the first order term of (9):

$$\delta f_{1,\mu}^{(\pm)}(k) = \frac{1}{\hbar} \frac{df_{01,\mu}^{(\pm)}}{dk} \frac{e \hat{E}_z}{\omega - v_{\mu}^{(\pm)} - i\nu}. \quad (9)$$

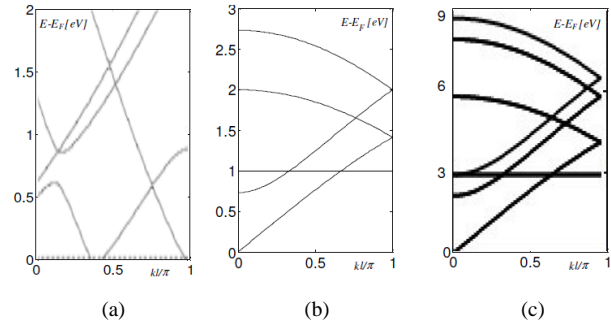


FIGURE 2 Energy band structure versus the normalized wavenumber $k' = kl / \pi$, for (a) copper NW, (b) metallic GNR, and (c) metallic CNT

Following the stream of what done in [30], the current density \hat{J}_z is expressed as:

$$\hat{J}_z(\beta, \omega) = \sum_{\mu=1}^N \int_{-\pi/l}^{+\pi/l} [e v_{\mu}^{(-)}(k) \delta f_{1,\mu}^{(-)}(k, \beta, \omega) + e v_{\mu}^{(+)}(k) \delta f_{1,\mu}^{(+)}(k, \beta, \omega)] dk. \quad (10)$$

The first term in the integral gives the contribution from to the valence bands, while the second term that from the conduction bands. In case of symmetry, the sum may be limited to the conduction subbands only, as done in [28] for CNTs and in [30] for GNRs.

By combining (9) and (10) we get:

$$\hat{J}_z(\beta, \omega) = \hat{\sigma}_{zz}(\beta, \omega) \hat{E}_z(\beta, \omega) s, \quad (11)$$

where the longitudinal conductivity in the wavenumber domain is given by the sum of all the contributions of the subbands:

$$\hat{\sigma}_{zz}(\beta, \omega) = \sum_{\mu=1}^N \hat{\sigma}_{\mu}, \quad (12)$$

$$\hat{\sigma}_{\mu} = i \frac{e^2}{\hbar} \int_{-\pi/l}^{+\pi/l} \left[\frac{v_{\mu}^{(-)}(k)}{\omega - v_{\mu}^{(-)}(k) \beta - i\nu} \frac{df_{0,\mu}^{(-)}}{dk} + \frac{v_{\mu}^{(+)}(k)}{\omega - v_{\mu}^{(+)}(k) \beta - i\nu} \frac{df_{0,\mu}^{(+)}}{dk} \right] dk. \quad (13)$$

The quantities $\hat{\sigma}_{\mu}$ are not, in general, of the same order of magnitude: only some of the subbands give a significant contribution to the conduction, those for which the energy gap with respect to the Fermi level E_F is such that $|E_{\mu} - E_F| \leq 5k_B T$. To catch in a simple way the main features of the dependence of $\hat{\sigma}_{zz}(\beta, \omega)$ on the wavenumber β and frequency ω , we assume that v_{μ} is approximately constant for all the subbands near the Fermi level, and hence:

$$\hat{\sigma}_{zz}(\beta, \omega) \cong -i \frac{2e^2 v_F}{\pi X \hbar} \frac{1}{\omega - i\nu} M \left[1 + \alpha \left(\frac{v_F \beta}{\omega - i\nu} \right)^2 \right] \quad (14)$$

and thus, from (14) and (11), we finally obtain the *generalized Ohm's law*

$$\left[1 - \psi(\omega) \beta^2 \right] \hat{J}_z(\beta, \omega) = \frac{\sigma_0}{1 + i\omega / \nu} \hat{E}_z(\beta, \omega). \quad (15)$$

In (14) and (15) we have introduced:

$$\psi(\omega) = \frac{\alpha(\omega)v_F^2}{v^2(1+i\omega/\nu)^2}, \quad \sigma_0 = \frac{2v_F M}{\nu R_0 X}, \quad (16)$$

being $R_0 = 12.9 \text{ k}\Omega$ the *quantum resistance*, and

$$M = \frac{\hbar}{v_F} \sum_{\mu=1}^N \int_0^{\pi/l} \left[v_{\mu}^{(+)} \left(-\frac{dF}{dE_{\mu}^{(+)}} \right) + v_{\mu}^{(-)} \left(-\frac{dF}{dE_{\mu}^{(-)}} \right) \right] dk. \quad (17)$$

Finally, the function $\alpha(\omega)$ is equal to 1 for CNTs [12], whereas for GNR it is

$$\alpha = \frac{\hbar}{Mv_F^3} \sum_{\mu=0}^{n-1} \int_0^{\pi/l} \left[v_{\mu}^{(+)} \left(-\frac{dF}{dE_{\mu}^{(+)}} \right) + v_{\mu}^{(-)} \left(-\frac{dF}{dE_{\mu}^{(-)}} \right) \right] dk \quad (18)$$

and for solid nanowires [36]:

$$\alpha(\omega) = \frac{1}{3} \frac{1+1.8i\omega/\nu}{1+i\omega/\nu}. \quad (19)$$

The interpretation of the generalized Ohm's law (14) is discussed in the next Section. Here we observe that the quantity M in (17) is the *equivalent number of conducting channels*, a measure of the number of subbands that effectively contribute to the electric conduction, i.e. those that cross or are closer to the Fermi level. In general, this number may be expressed as

$$M = \xi X N_{DOS}, \quad (20)$$

where ξ is a material constant, X is defined in (7) and N_{DOS} is the total number of available states, which are related to the density of states. A detailed discussion on the behavior of such number M for CNTs and GNRs may be found in [28, 30, 37, 38], where it is clearly shown how such a quantity strongly depends on the chirality, size and temperature of such carbon nanostructures. Here we compare the number of channels for metallic CNTs, GNRs and Cu nanowires, assuming $T = 300 \text{ K}$, with varying dimensions. The results shown in Table 1 highlights the strong difference between conventional materials and carbon-based ones: as the cross section dimension increases, the number of subbands contributing to the conduction exhibits a limited increase for CNTs and GNRs, whereas for conventional metals such a number experience a steep increase. In other words, for CNTs and GNRs the energy levels may be assumed to be quantized for transverse dimensions up to some hundreds of nm, whereas for nanowires of conventional metals this phenomenon only happens for dimensions of the order of tens of nm or lower.

TABLE 1 Number of conducting channels for metallic NW, GNR and CNT at 300 K

	1 nm	10 nm	50 nm	100 nm
CNT	2.00	2.12	5.04	9.93
GNR	1.00	1.07	1.57	3.13
NW	3.12	11.75	220.98	874.82

3 Propagation properties of nano-interconnects

In this Section we investigate the generalized Ohm's law (14) and its impact in the properties of the electrical propagation

along the nano-interconnects of Figure 1.

3.1 GENERALIZED TRANSMISSION LINE MODEL

By using the charge conservation law, Eq. (16) may be rewritten in frequency domain as follows:

$$I(z, \omega) - i\omega\psi(\omega) \frac{\partial I(z, \omega)}{\partial z} = \frac{\sigma_0 X}{1+i\omega/\nu} E_z(z, \omega), \quad (21)$$

where the second term in the l.h.s introduces a spatial and frequency dispersion, whereas the coefficient of the electric field introduces a frequency dispersion.

By coupling (21) to the Maxwell equations, in the low bias condition and for operating frequencies up to the order of THz, it is possible to derive a simple transmission line model for the nano-interconnects schemes in Figure 1. The details of such a derivation are given in [28-30]. The final expressions for the a transmission line per-unit-length resistance, inductance and capacitance are given by:

$$R_{TL} = \frac{\nu L_k}{\Theta(\omega)}, \quad L_{TL} = \frac{L_k + L_m}{\Theta(\omega)}, \quad C_{TL} = C_e, \quad (22)$$

where L_m and C_e are the p.u.l. magnetic inductance and electrostatic capacitance, and

$$L_k = \frac{1}{\nu\sigma_0 X}, \quad \Theta(\omega) = 1 + \frac{C_e}{C_q} \frac{\alpha}{1-i\nu/\omega}, \quad C_q = \frac{\nu_F^2}{L_k}. \quad (23)$$

The p.u.l. *kinetic inductance* L_k takes into account the effects of the mass inertia of the conduction electrons, whereas the p.u.l. *quantum capacitance* C_q is related to the effects due to the quantum pressure arising from the zero-point energy of such electrons.

The parameters of the TL model (24) generalize those given for the classical TL model, which can be viewed as the limit of (24) when the effects of the kinetic inductance and the quantum capacitance are negligible. Let us for instance consider the simple interconnect of Figure 1a, assuming the signal trace to be made by bulk copper, with a radius of 100 nm and distance to the ground of 400 nm. For such dimensions and assuming room temperature, the number of conducting channel is $M \approx 3.1 \cdot 10^5$, which provides the bulk copper DC conductivity of $\sigma_0 \approx 6 \cdot 10^7 \text{ S/m}$ and leads to the p.u.l. parameters reported in Table 2. Given these values, it is easy to show that $\Theta \approx 1$ and $L_k \ll L_m$, and so the expressions in (24) reduce to the classical ones:

$$R_{TL} = \frac{1}{\sigma_0 X}, \quad L_{TL} = L_m, \quad C_{TL} = C_e. \quad (24)$$

This means that the quantum, kinetic and dispersive effects introduced in (22) are experienced only for smaller sizes, when the density of states and consequently the number of conducting channels M drops down dramatically, as discussed in Section 2.

TABLE 2 P.u.l. parameters for the line in Figure 1a, made by bulk copper

L_m [nH/mm]	L_k [nH/mm]	C_e [fF/mm]	C_q [fF/mm]
0.42	0.01	26.7	$3 \cdot 10^7$

3.2 PROPAGATION PROPERTIES

The propagation properties of the nano-interconnects in Figure 1 may be investigated starting from the TL p.u.l. parameters (24) and deriving the longitudinal propagation wavenumber, defined as:

$$k_{TL}(\omega) = \alpha_{TL}(\omega) + i\beta_{TL}(\omega) = \sqrt{(R_T + i\omega L_T)i\omega C_T}, \quad (25)$$

In particular, it is useful to study the normalized phase velocity $\beta_{TL}(\omega)$, i.e. the phase velocity compared to the value obtained if the line were made by ideal perfect conductor, $k_0 = i\omega\sqrt{L_m C_e}$. The real part $\alpha_{TL}(\omega)$ in (25), instead, is the attenuation constant, and gives a measure of the damping and dispersion of the signal introduced by the losses.

Let us consider two case-studies: the first refers to an on-chip local level interconnect at the 14 nm node [17], for which we assume, according to Fig.1, $D = W = 14$ nm, $t = 2D$ and a dielectric constant of the embedding medium $\epsilon_r = 2.2$. Let us consider room temperature and let us assume the signal conductor of Fig.1 to be made by a metallic single-wall CNT, a metallic GNR and a copper NW. The second case study refers to the same arrangements and conditions, but with $D = W = 1$ nm.

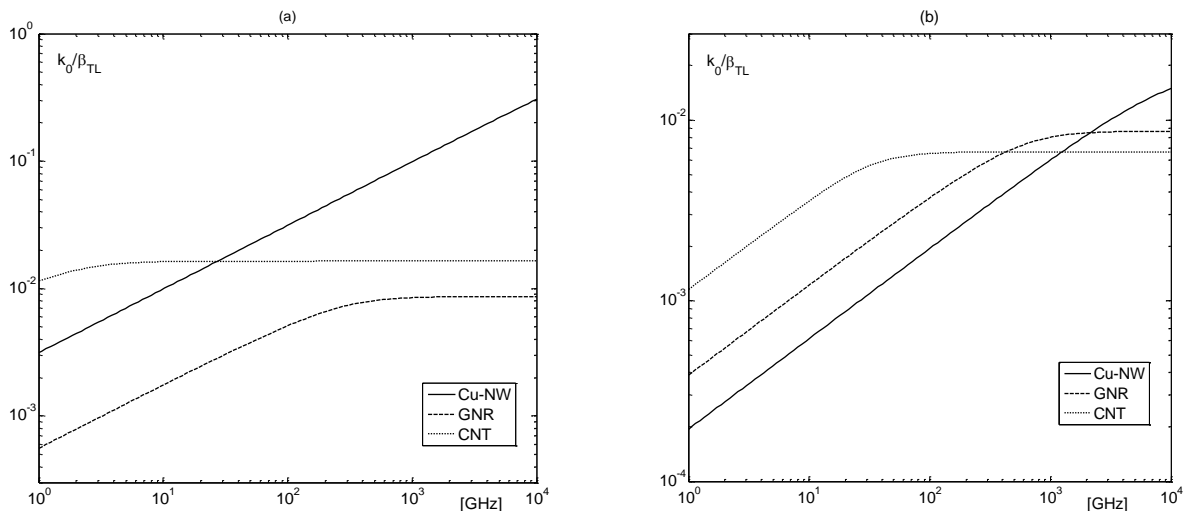


FIGURE 3 Dispersion in the normalized phase velocity for an on-chip interconnect of width of: (a) 14 nm; (b) 1 nm

5 Conclusions

A general frame has been derived to study the propagation of electrical signals along nano-interconnects made by 1D materials, in low bias conditions and for frequencies up to THz. A semi-classical model for the electrodynamics allows writing a generalized Ohm's law to describe the relation between the density of current and the electric field.

The propagation properties of such interconnects have been investigated, showing that the dispersion phenomena affect in different way the carbon-based interconnects and those made by conventional metals, arranged in nanowires. A crucial role is played by the different behavior of the number of conducting channels, which exhibits a strong

dependence on the quantization in the transverse direction. Such an effect is observed in graphene and carbon nanotubes with transverse sizes up to hundreds nanometers, whereas the nanowires exhibits a low number of conducting channels only up to some tens of nanometers.

As a consequence, the propagation velocity for carbon-based interconnects is 1-2 order of magnitude smaller than the ideal one, whereas that of nanowires of conventional materials is close to the ideal one, unless for transverse dimensions smaller than 10 nanometers. This provides a physical explanation of a well-known result for the carbon nanotubes and graphene nanoribbons.

Figure 3 shows the normalized phase velocity $k_0/\beta_{TL}(\omega)$, for the two case-studies. The different dispersion introduced by the generalized Ohm's law, leads to saturation in different frequency ranges. In all cases, the carbon line velocity saturates to a value that is two orders of magnitude smaller than the ideal velocity. This is a well-known consequence of the role played by the kinetic inductance [21-31]. For case-study 1 the copper line is not evidently affected by the quantum effects, and so its phase velocity exhibits a behavior similar to bulk copper, with saturation close to the ideal velocity.

In case-study 2, the copper line behaves like the carbon ones, exhibiting the same slowing down of velocity. The reason for this behavior is given in Table 1, from which it is clear that copper nanowires start to experience the effect of the transverse quantum confinement only for dimensions below 10 nanometers.

Figure 4 shows the dispersion for the attenuation constant $\alpha_{TL}(\omega)$, i.e. the frequency behavior of the losses. The attenuation introduced by CNTs is lower than the other two realizations and is almost constant over the considered frequency range. As expected, the attenuation introduced by the copper NW is increasing with frequency increasing, and is generally lower than the one introduced by GNRs for 14 nm, whereas for 1 nm the performance of Cu-NW is the worst one.

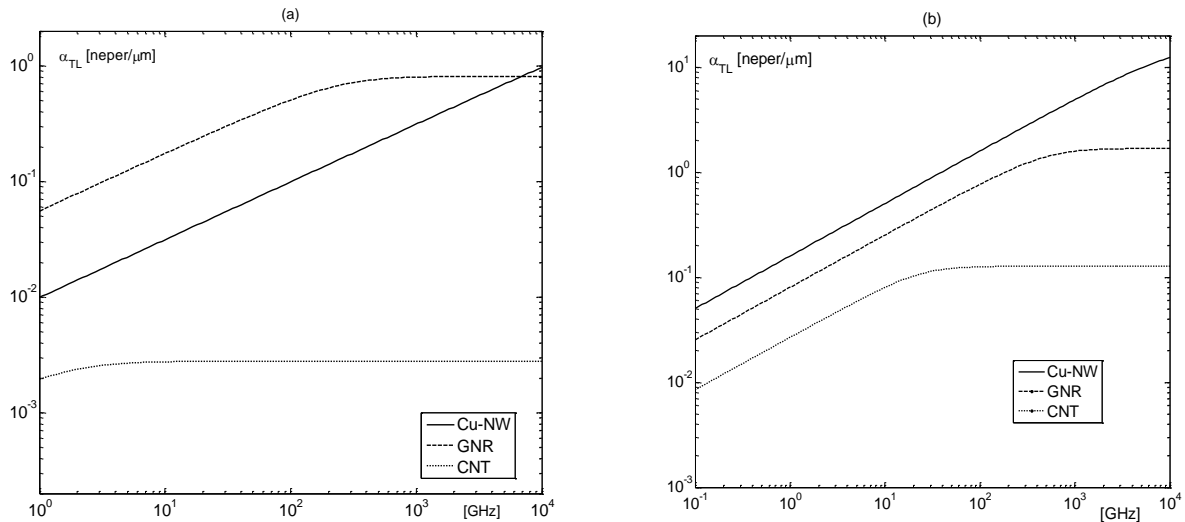


FIGURE 4 Dispersion in the attenuation constant for an on-chip interconnect of width of: (a) 14 nm; (b) 1 nm

As for the attenuation, the carbon interconnects exhibit a saturation phenomena, which means that in a subrange of the investigated frequency range this attenuation is constant. This is more evident in carbon nanotubes, for which the

attenuation values are also the best. Also in this case, moving from 14 nm to 1 nm, the copper nanowire exhibits a strong degradation of its performance.

References

- [1] Saito R, Dresselhaus G., Dresselhaus M S 2004 *Physical Properties of Carbon Nanotubes* Imperial College Press: Singapore
- [2] Castro Neto A H, Guinea F, Peres N M R, Novoselov K S, K. Geim A K 2009 *Reviews of Modern Physics* **81** 109
- [3] Avouris P, Chen Z, Perebeinos V 2007 *Nature Nanotech.* **2** 605
- [4] Van Noorden R 2006 *Nature* **442** 228
- [5] Li Y, Zhang X B, Tao X Y, Xu J M, Huang W Z, Luo J H, Luo Z Q, Li T, Liu F, Bao Y, Geise H J 2005 *Carbon* **43** 295
- [6] Li X, Cai W, An J, Kim S, Nah J, Yang D, Piner R, Velamakanni A, Jung I, Tutuc E, Banerjee S K, Colombo L, and Ruoff R S 2009 *Science* **324** 1312
- [7] Zhou Y, Sreekala S, Ajayan P M, Nayak S K 2008 *J. Phys. Cond. Matter* **20** 095209
- [8] Geim A K 2009 *Science* **324** 1530
- [9] Naeemi A, Meindl J D 2008 *IEEE Trans. Electron Devices* **55** 2574
- [10] Maffucci A, Miano G, Villone F 2008 *IEEE Trans. on Advanced Packaging* **31** 692
- [11] Li H, Xu C, Srivastava N, Banerjee K 2009 *IEEE Trans. on Electron Devices* **56** 1799
- [12] Cui J-P, Zhao W-S, Yin W-Y, Hu J 2012 *IEEE Trans. on Electromagnetic Compatibility* **54** 126.
- [13] Close G F, Yasuda S, Paul B, Fujita S, Philip Wong H-S 2009 *Nano Letters* **8** 706
- [14] Chen X, Akinwande D, Lee K-J, Close G F, Yasuda S, Paul B C, Fujita S, Kong J, Philip Wong H-S 2010 *IEEE Trans. Electr. Devices* **57** 3137
- [15] Shulaker M M, Hills G, Patil N, Wei H, Chen H-Y, Philip Wong H-S, Mitra S 2013 *Natur* **501** 526
- [16] Valitova I, Amato M, Mahvash F, Cantele G, Maffucci A, Santato C, Martel R, Coiro F 2013 *Nanoscale* **5** 4638
- [17] International Technology Roadmap for Semiconductors 2011 <http://public.itrs.net>.
- [18] Tseng G Y, Ellenbogen J C 2001 *Science* **294** 1293
- [19] Joachim C, Gimzewski J K, Aviram A 2000 *Nature* **408** 541
- [20] Morris J E 2008 *Nanopackaging: Nanotechnologies and electronics packaging* Springer: New-York, USA
- [21] Burke P J 2002 *IEEE Trans. Nanotechnology* **1** 129
- [22] Salahuddin S, Lundstrom M, Datta S 2005 *IEEE Trans. Electron. Devices* **52** 1734
- [23] Xu C, Li H, Banerjee K 2009 *IEEE Trans. Electron Devices* **56** 1567.
- [24] Zhao W-S, Yin W-Y, Guo Y-X 2012 *IEEE Trans. on Electromagnetic Compatibility* **54** 149
- [25] Maffucci A, Miano G 2013 *IEEE Trans. Components, Packaging and Manufacturing Technology* **3** 1926.
- [26] Naeemi A and Meindl J D 2009 *IEEE Trans. Electron Dev.* **56** 1822
- [27] Maffucci A, Miano G, Villone F 2009 *IEEE Trans. Nanotechnology* **8** 345
- [28] Miano G, Forestiere C, Maffucci A, Maksimenko S A, Slepian G Y 2011 *IEEE Transactions on Nanotechnology* **10** 135
- [29] Forestiere C, Maffucci A, Maksimenko S A, Miano G., Slepian G Y 2012 *IEEE Transactions on Nanotechnology* **11** 554
- [30] Maffucci A, Miano G 2013 *Nanoscience and Nanotechnology Letters* **5** 1207
- [31] Forestiere C, Maffucci A, Miano G 2010 *Journal of Nanophotonics* **4** 041695
- [32] Zheng H, Wang Z F, Luo T, Shi Q W, Chen J 2007 *Physical Review B* **75** 165414
- [33] Moradinab M, Nematian H, Pourfath M, Fatipour M, Kosina H 2012 *Journal of Applied Physics* **111** 074318
- [34] Wakabayashi K, Sasaki K, Nakanishi T, Enoki T. 2010 *Sci. Technol. Adv. Mater.* **11** 054504
- [35] Zhou Y, Sreekala S, Ajayan P M, Nayak S K, 2008 *J. Phys. Cond. Matter* **20** 095209
- [36] Hanson G W 2011 *IEEE Trans. Microwave Theory and Tech.* **59** 9
- [37] Forestiere C, Maffucci A, Miano G 2011 *IEEE Transactions on Nanotechnology* **10** 1221.
- [38] Maffucci A, Miano G 2013 *IEEE Trans. Nanotechnology* **12** 817

Authors	
	<p>Antonio Maffucci</p> <p>Current position: Associate Professor University studies: M.Sc. Electronic Engineering, PhD in Electrical Engineering Scientific interest: electromagnetic modeling, electromagnetic compatibility, computational electromagnetism and nanotechnology Publications: about 160 papers in international journals and conference proceedings, 1 book: "Transmission Lines and Lumped Circuits", 2001, Academic: New York. Experience: University of Naples Federico II (Italy); JET – Culham (UK)</p>
	<p>Giovanni Miano</p> <p>Current position: Full professor University studies: M.Sc. Electronic Engineering, Ph.D. Electrical Engineering Scientific interest: ferromagnetic materials, nonlinear dielectrics, plasmas, electrodynamics of continuum media, nanotechnology and modeling of lumped and distributed circuits. Publication: about 200 papers in international journals and conference proceedings, 1 book: "Transmission Lines and Lumped Circuits", 2001, Academic: New York. Experience: University of Naples Federico II (Italy); GSI, Darmstadt (Germany); University of Maryland (USA).</p>